$O_2(a\ ^1\Delta_g)$ production in flowing $Ar-O_2$ surface-wave microwave discharges: Possible use for oxygen-iodine laser excitation

Vasco Guerra,[1] Kinga Kutasi,[2,a)] and Paulo A. Sá[3]
[1]*Instituto de Plasmas e Fusão Nuclear, Instituto Superior Técnico, 1049-001 Lisboa, Portugal*
[2]*Research Institute for Solid State Physics and Optics, Hungarian Academy of Sciences, P.O. Box 49, H-1525 Budapest, Hungary*
[3]*Instituto de Plasmas e Fusão Nuclear, Instituto Superior Técnico, 1049-001 Lisboa, Portugal and Departamento de Engenharia Física, Faculdade de Engenharia da Universidade do Porto, 4200-465 Porto, Portugal*

(Received 15 December 2009; accepted 25 January 2010; published online 18 February 2010)

Herein we present the calculations conducted on an $Ar-O_2$ surface-wave microwave discharge and its afterglow, and show that this system can be effectively used for the oxygen-iodine laser excitation. It is demonstrated that at pressures higher than 10 mbar $O_2(a)$ yields higher than the threshold yield required for positive gain can be achieved along the afterglow. Additionally, the density of $O(^3P)$ atoms, which can quench the $I(^2P_{1/2})$ excited state, can be tuned to the desired level. © *2010 American Institute of Physics*. [doi:10.1063/1.3318253]

The classical chemical oxygen-iodine laser operates on the electronic transition of the iodine atom at 1315 nm, where the population of the upper state $I(^2P_{1/2})$ occurs in the reaction of chemically generated singlet oxygen metastable $O_2(a\ ^1\Delta_g)$ with I_2. Due to logistic problems with the chemical $O_2(a\ ^1\Delta_g)$ generator, attention has been turned to a simpler system, in which $O_2(a\ ^1\Delta_g)$ is produced in a stable discharge, i.e., the electric discharge oxygen-iodine laser (DOIL) as demonstrated by Carroll *et al.*[1] Carroll *et al.* suggest that in $O_2(a)$ and O containing plasmas I_2 is dissociated mostly by O atoms (the O atom reacting with I_2 gives rise to IO, which is subsequently dissociated in collisions with O). Thus, negligible $O_2(a)$ is consumed in I_2 dissociation. Furthermore, excited I^* is produced in the $O_2(a)+I \rightarrow O_2(X)+I^*$ process. Due to this excitation mechanism, population inversion in the transition $I^*(^2P_{1/2}) \rightarrow I(^2P_{3/2})$ takes place when the $O_2(a)$ concentration satisfies the condition $[O_2(a)]/[O_2(X)]=Y>1/2K_{eq}$, where $[O_2(X)]$ is the concentration of ground state oxygen molecule, the equilibrium constant K_{eq} is the ratio of rate constants of forward and backward processes, and Y is the $O_2(a)$ yield. This expression is derived from the condition of inversion population arising in the iodine atom, $[I^*(^2P_{1/2})]>0.5[I(^2P_{3/2})]$, and the equilibrium equation in the atomic iodine-oxygen system, $K_{eq}[O_2(a)]/[O_2(X)]=[I^*(^2P_{1/2})]/[I(^2P_{3/2})]$.[2] According to Rawlins *et al.*[3] the equilibrium constant is $K_{eq}=0.75\ \exp(402/T)$. Hence, in order to achieve a positive gain the yield of $O_2(a)$ should be at least equal to the threshold yield, $Y_{th}=1/2K_{eq}$, which at 400 K is 24%.

In the last few years several discharge systems have been suggested and investigated, where yields around and higher than Y_{th} have been achieved.[2–7] In these investigations it has also been shown that oxygen atoms can quench the desired $I(^2P_{1/2})$ state,[8,9] which may lead to a decrease in the gain. To reduce the O-atoms density, addition of NO to the plasma has been considered,[4] since NO is able to remove the O-atoms. Woodard *et al.* have observed a considerable increase of the gain when NO has been added to the discharge mixture.[4]

Here we propose a system, based on the afterglow of a flowing surface-wave microwave discharge, where high $O_2(a)$ yields can be achieved. In turn, the O-atoms density can be adjusted by using different regions of the flowing afterglow plasma, as the atoms recombine along the afterglow, and/or by tuning the O-atoms losses in the afterglow through surface recombination, which is one of the main loss channels of O-atoms. The atomic surface recombination depends on the wall temperature and the surface material.[10,11] Thus, the O-atoms density can be changed by varying the wall temperature, the size of the afterglow tube or by using different tube materials.

The source of active species is a surface-wave microwave discharge generated with a surfatron in an $Ar-O_2$ mixture in a quartz tube of 1 cm diameter. A detailed description of this type of discharges can be found in Refs. 12 and 13. The microwave field frequency used is $\omega/2\pi=2.45$ GHz. The gas flow applied carries the species generated in the discharge along an afterglow tube, which can have either the diameter of the discharge tube or differ from it, depending on the purpose of the application. Our goal is to find the conditions favorable for the oxygen-iodine laser excitation. To this purpose, the species densities are determined in the discharge and along the afterglow by plasma modeling.

The surface-wave microwave discharge is described with a zero-dimensional kinetic model that is based on the solutions of the electron Boltzmann equation in local approximation for the microwave field, coupled to a system of rate-balance equations for the neutral and charged heavy species (for more details the reader should refer to Refs. 14 and 15 where the gas phase and surface reactions taken into account in the model are also listed). Despite the importance of nonlocal effects in several discharge systems,[16] for the discharge type and pressure range under analysis here the local approximation is well justified.

A surface wave microwave discharge is a plasma column with a decreasing electron density profile, as discussed in Refs. 12 and 13. At the end of plasma column the electron

a)Electronic mail: kutasi@mail.kfki.hu.

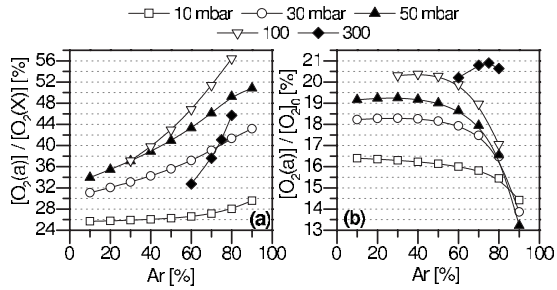

FIG. 1. (a) $Y=[O_2(a)]/[O_2(X)]$ yield and (b) $[O_2(a)]/[O_2]_0$ ratio at the end of the discharge as a function of Ar percentage for different pressures.

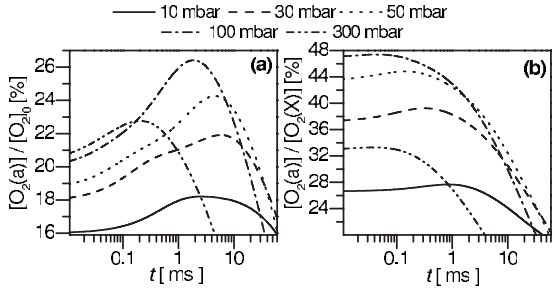

FIG. 2. (a) $[O_2(a)]/[O_2]_0$ ratio and (b) $O_2(a)$ yield as a function of flight time of species in the afterglow for 60%Ar–O_2 initial mixture composition.

density reaches the value of n_{ec} the critical density for surface wave mode propagation in a homogeneous, cold, collisionless plasma, surrounded by a dielectric of permittivity ϵ_g. The surface wave mode can only propagate provided the electron density is larger than this critical value, obtained from $\omega_{pe} > \omega\sqrt{1+\epsilon_g}$, with ω_{pe} denoting the electron plasma angular frequency, which for a quartz tube ($\epsilon_g=4$) gives $n_{ec}=3.74\times10^{11}$ cm^{-3} at 2.45 GHz. Our calculations for the discharge zone are conducted for this critical electron density, so that the species densities are obtained at the end of the plasma column. The so obtained species densities serve as input data for the afterglow model, which describes the evolution of species densities downstream the discharge along the afterglow tube. The afterglow model is based on the same rate-balance equations as the discharge model, however in the afterglow the excitation by electron impact is neglected. The correctness of the present model has been shown in Ref. 15, where a very good agreement between calculated and experimental results has been found for a variety of conditions.

The calculations have been carried out in a wide range of pressure, 1–300 mbar, in mixtures from pure O_2 to 90%Ar–O_2. The $O_2(a)$ yield, $Y=[O_2(a)]/[O_2(X)]$, the $[O_2(a)]/[O_2]_0$ ratio—with $[O_2]_0$ being the initial density of O_2 in the mixture—and the atomic concentration have been determined at the end of the discharge and along the afterglow.

Figure 1(a) shows the yield at the end of the discharge as a function of the Ar percentage in the initial mixture composition for different pressure values. In the 10–300 mbar pressure range the lowest yield is obtained at 10 mbar, while the highest yield occurs at 100 mbar. At 10 mbar in a mixture with 10% Ar the yield is about 25%, which is already higher than the threshold yield required for positive gain, $Y_{th}=24\%$. The yield still increases with the Ar percentage, which is related to the increase of O_2 dissociation with Ar addition. In fact, O_2 is effectively dissociated by the Ar 4*s* atoms, resulting in the decrease in the $O_2(X)$ density.[15] As a consequence, the highest yields are obtained in high Ar contain mixtures, the highest yield here observed is 56%, obtained at 100 mbar in 80%Ar–O_2. A value higher than 50% is also achieved at 50 mbar in 90%Ar–O_2.

It is interesting to note that at the highest pressure here investigated, 300 mbar, the yield is lower than at 50 mbar and, depending on the mixture composition, can also be lower than at 30 mbar. This occurs due to the decrease in O_2 dissociation degree, and thus an increase in $O_2(X)$ relative density (relative to O_2 initial density). At the same time, the $O_2(a)$ relative density also increases as shown in Fig. 1(b), where $[O_2(a)]/[O_2]_0$ is presented. This figure reveals that the highest $O_2(a)$ relative density can be achieved at 300 mbar in 80%Ar–O_2, whereas at lower pressures the maximum of the $O_2(a)$ relative density occurs in mixtures with smaller Ar content.

As it was already suggested, the application zone of the system is the flowing afterglow of a surface-wave microwave discharge. Due to the recombination of atoms along the afterglow the yields obtained at the end of the discharge change along the afterglow. Figure 2 depicts the evolution of the yield and the $[O_2(a)]/[O_2]_0$ ratio along an afterglow tube for 60%Ar–O_2 initial mixture composition. Data are presented as a function of the flight-time of species in the afterglow, determined at a given pressure and discharge tube radius by the gas flow. Figure 2(a) shows that the $O_2(a)$ relative density has a maximum in the afterglow that occurs around 10 ms at 30 mbar, and is shifted to earlier times as the pressure increases, taking place at 0.3 ms at 300 mbar. The $O_2(a)$ yield, $[O_2(a)]/[O_2(X)]$, shows also a maximum in the afterglow, however it occurs earlier. Furthermore, the increase in the yield at the beginning of the afterglow is smaller compared to that of $[O_2(a)]/[O_2]_0$. The increase of the $O_2(a)$ density in the afterglow is related with the de-excitation of $O_2(b)$ to $O_2(a)$.

The oxygen atomic density can be controlled in several ways. Here, we present the effect of the surface recombination probability and of the tube radius. The former can be varied by changing the surface temperature and/or the wall material. Figure 3 shows the $O(^3P)$ atom and $O_2(a)$ densities, as well as the yield as a function of the afterglow time at 50 mbar in 50%Ar–O_2 mixture for three different conditions

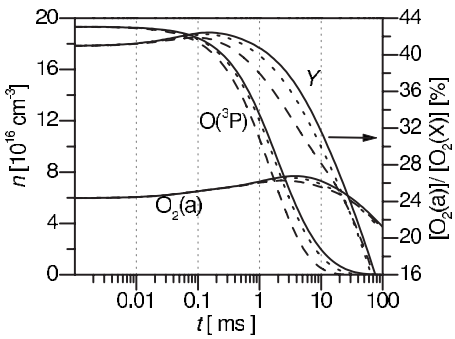

FIG. 3. $O(^3P)$ and $O_2(a)$ densities (left axis), and yield (right axis) as a function of afterglow time at 50 mbar in 50%Ar–O_2 mixture for: $R=0.5$ cm and $\gamma=10^{-3}$ (full line), $R=0.5$ cm and $\gamma=10^{-2}$ (dashed) and $R=0.25$ cm and $\gamma=10^{-3}$ (dotted).

concerning the afterglow tube radius R and the O-atoms surface recombination probability γ as follows: (i) $R=0.5$ cm and $\gamma=10^{-3}$, (ii) $R=0.5$ cm and $\gamma=10^{-2}$, and (iii) $R=0.25$ cm and $\gamma=10^{-3}$. As shown in the figure, the decrease in the atomic concentration due to recombination starts to be noticeable at about 0.1 ms in the afterglow, the atomic density dropping two orders of magnitude in 10 ms. Meanwhile, the $O_2(a)$ density peaks at about 1–10 ms and decreases slowly after 20 ms. Notice that at about 2 ms the $O_2(a)$ and $O(^3P)$ densities become equal. At this high pressure the decrease in the tube radius has a lower effect on the $O(^3P)$ density than the increase in the surface recombination probability. An increase in one order of magnitude in the surface recombination probability produces a decrease in about a factor of 2 in the atom density. Due to the decrease in the $O(^3P)$ density a minor change can be observed also in the $O_2(a)$ density, and, as a consequence of the increase of the $O_2(X)$ density, a somewhat more pronounced variation on the $O_2(a)$ yield.

Our calculations have shown that the $O_2(a)$ threshold yield necessary for positive gain can be achieved at 10 mbar, the yield increases with pressure until it reaches a maximum of about 56% at 100 mbar, being already as high as 50% at 50 mbar. It has also been shown that the yield increases with Ar addition into O_2, as a result of the increase in O_2 dissociation with the Ar percentage. Moreover, the yield and the $[O_2(a)]/[O_2]_0$ ratio have a maximum in the afterglow between 1 and 10 ms, depending on the pressure. It was further demonstrated that the O-atoms density can be tuned to the desired level in the afterglow. At the same time, O_3, that was also named as a possible quencher of the $I(^2P_{1/2})$ state, has a density of three to four orders of magnitude lower than that of $O(^3P)$.

The work has been supported by Hungarian OTKA Project F-67556 and by Janos Bolyai Scholarship of HAS, and the Portuguese FCT funds to IPFN-LA.

[1]D. L. Carroll, J. T. Verdeyen, D. M. King, J. W. Zimmerman, J. K. Laystrom, B. S. Woodard, N. Richardson, K. Kittell, M. J. Kushner, and W. C. Solomon, Appl. Phys. Lett. **85**, 1320 (2004).
[2]A. A. Ionin, I. V. Kochetov, A. P. Napartovich, and N. N. Yuryshev, J. Phys. D: Appl. Phys. **40**, R25 (2007).
[3]W. T. Rawlins, S. Lee, W. J. Kessler, and S. J. Davis, Appl. Phys. Lett. **86**, 051105 (2005).
[4]B. S. Woodard, J. W. Zimmerman, G. F. Benavides, D. L. Carroll, J. T. Verdeyen, A. D. Palla, T. H. Field, W. C. Solomon, S. J. Davis, W. T. Rawlins, and S. Lee, Appl. Phys. Lett. **93**, 021104 (2008).
[5]A. Hicks, S. Tirupathi, N. Jiang, Yu. Utkin, W. R. Lempert, J. W. Rich, and I. V. Adamovich, J. Phys. D: Appl. Phys. **40**, 1408 (2007).
[6]G. F. Benavides, J. W. Zimmerman, B. S. Woodard, D. L. Carroll, J. T. Verdeyen, T. H. Field, A. D. Palla, and W. C. Solomon, Appl. Phys. Lett. **92**, 041116 (2008).
[7]J. Schmiedberger, V. Jirasek, J. Kodymova, and K. Rohlena, Eur. Phys. J. D **54**, 239 (2009).
[8]V. N. Azayazov, I. O. Antonov, S. Ruffner, and M. C. Heaven, Proc. SPIE **6101**, 61011Y (2006).
[9]D. L. Carroll, J. T. Verdeyen, D. M. King, J. W. Zimmerman, J. K. Laystrom, B. S. Woodard, G. F. Benavides, K. Kittell, and W. C. Solomon, IEEE J. Quantum Electron. **41**, 213 (2005).
[10]K. Kutasi and J. Loureiro, J. Phys. D: Appl. Phys. **40**, 5612 (2007).
[11]M. Shibata, N. Nakano, and T. Makabe, J. Appl. Phys. **80**, 6142 (1996).
[12]E. Tatarova, F. M. Dias, C. M. Ferreira, and A. Ricard, J. Appl. Phys. **85**, 49 (1999).
[13]C. M. Ferreira, E. Tatarova, V. Guerra, B. F. Gordiets, J. Henriques, F. M. Dias, and M. Pinheiro, IEEE Trans. Plasma Sci. **31**, 645 (2003).
[14]C. D. Pintassilgo, J. Loureiro, and V. Guerra, J. Phys. D: Appl. Phys. **38**, 417 (2005).
[15]K. Kutasi, V. Guerra, and P. Sá, "Theoretical insight into surfatron generated Ar–O_2 surface-wave microwave discharges," J. Phys. D: Appl. Phys. (to be published).
[16]Z. L. Petrović, M. Šuvakov, Ž. Nikitović, S. Dujko, O. Šašić, J. Jovanović, G. Malović, and V. Stojanović, Plasma Sources Sci. Technol. **16**, S1 (2007).